Contrib Mineral Petrol (2003) 144: 559–569
DOI 10.1007/s00410-002-0414-1

ORIGINAL PAPER

Robin F. Preston · Gary Stevens · Terence S. McCarthy

Fluid compositions in equilibrium with silica-undersaturated magmas in the system Na_2O–Al_2O_3–SiO_2–H_2O: clues to the composition of fenitizing fluids

Received: 12 October 2000 / Accepted: 4 September 2002 / Published online: 7 November 2002

Abstract Fenites result from alkali metasomatism of granitoid rocks associated with the intrusion of silica-undersaturated alkaline magmas, and are characterized by addition of alkalis, iron and magnesium, albitization, nephelinization, removal of silica and the formation of alkali pyroxenes and amphiboles. In an attempt to constrain the fluid compositions involved in this process, we have investigated the compositions of the fluids in equilibrium with a range silica-undersaturated alkaline magmas, in the model system Al_2O_3–Na_2O–SiO_2–H_2O at 850 °C and 1 kbar. The starting compositions straddle the nepheline–albite join, and include both peralkaline and alkali-granitoid compositions. The quenched run products all contained a glass, representing the melt, as well as an aqueous fluid and a radial crystalline phase interpreted to be a fluid quench phase. Several of the glasses also contained albite, nepheline or quartz crystals. Fluid compositions in crystal-free experiments were calculated using a mass-balance approach that incorporated the composition of the glass, composition of starting materials and carefully determined masses of the different run product fractions, as well as that of the starting materials. Compositions plotting to the peralkaline side of the nepheline–albite join produced fluids that were highly enriched in dissolved solids (SiO_2 + Al_2O_3 + Na_2O, in the range 40–50 wt%). This substantial fractionation of the solid starting materials, between melt and fluid phase, results in reasonable resolution of the fluid compositions produced, despite significant uncertainties in the measured Na_2O and H_2O concentrations in the glasses. Model calculations indicate that the fluid compositions in equilibrium with the more SiO_2 undersaturated melt compositions in this study are capable of converting a typical granodiorite to a nepheline syenite composition at fluid/rock ratios lower than 1:1. Albitization and the removal of quartz (in the form of soluble sodium metasilicate), formation of sodic pyroxenes (acmite) and ultimately nepheline are characteristic of the process modeled here. These are largely analogous to the general features observed in some natural fenites.

R.F. Preston
Economic Geology Research Institute,
University of the Witwatersrand,
Private Bag 3, P.O. Wits 2050, South Africa

G. Stevens (✉)
Department of Geology, University of Stellenbosch,
Private Bag X1, 7602 Matieland, South Africa
E-mail: gs@land.sun.ac.za

T.S. McCarthy
Department of Geology, University of the Witwatersrand,
Private Bag 3, P.O. Wits 2050, South Africa

Editorial responsibility: T.L. Grove

Introduction

Fenites are metasomatic rocks characterized by the pervasive change of a (commonly granitoid) protolith to a more alkaline, silica undersaturated composition by fluids originating from alkaline silicate of carbonate magmas (Sindern and Kramm 2000). Results from numerous studies published over the last 80 years on this metasomatism have documented the mineralogical (e.g. McKie 1966; Cooper 1971; Currie 1971; Currie and Ferguson 1971, 1972; Siemiatkowska and Martin 1975; Vartiainen and Woolley 1976; Robins and Tysseland 1983; Garson et al. 1984; Robins 1984; Kresten and Morogan 1986; Le Bas 1987; Morogan and Woolley 1988; Gittins 1989; Currie et al. 1992; Morogan 1994; Pearson and Taylor 1996) and geochemical (e.g. Von Eckermann 1948; Strauss and Truter 1950; Saether 1957; McKie 1966; Verwoerd 1966; Vartiainen and Woolley 1976; Appleyard and Woolley 1979; Rubie 1982, Kresten 1988; Morogan 1994) changes induced by the process. Despite this good knowledge of the characteristics of fenitized rocks, the composition of the fluid phase that drives the process is far less well understood. Experimental studies represent one of the few means of directly determining the composition of the fluids

involved in fenitization, but owing to the technical difficulties associated with this approach, very little data exist. Typically, in experiments of this type, the sample volumes are extremely small, isochemical quenching of equilibrium run products is impossible and, consequently, the fluid phase retrieved from the capsule is not normally representative of the fluid that existed with the magma at high pressure and temperature. Despite these difficulties, an experimental approach may represent the best technique for quantifying the composition of fenitizing fluids, particularly so when it is considered that 80 years of study on natural rocks have not answered this specific question. The aims of this study are to investigate the equilibrium compositions of melts and fluids in the relevant portions of the system Na_2O–Al_2O_3–SiO_2–H_2O, and to use the derived fluid compositions to model the process of fenitization around syenitic intrusions, where this is likely to have the most relevance.

Previous work

Fenites were first described by Brögger (1921), in his pioneering work on the rocks of the Fen Complex in southern Norway. He defined fenites as a suite of rocks of originally granitic composition that had been metasomatically altered towards an alkali-syenitic composition by solutions sourced from an ijolite–melteigite magma within the complex. The term 'fenite' has since taken on a more general connotation, and encompasses a wide spectrum of generally alkaline alteration products developed within the immediate environs of silica-undersaturated, alkaline intrusions. Together with other workers (e.g. Currie and Ferguson 1971; Gittins 1989), McKie (1966) stated that fenites are normally associated with alkaline igneous intrusions containing carbonatite, and are manifest as an aureole of metasomatized rocks, grading outward from rocks indistinguishable from alkaline igneous varieties, implying that the development of fenites is intimately related to secondary processes operating within and around carbonatite complexes. According to Gittins (1989), fenitizing fluids are derived principally from carbonatite rather than ijolite or nephelinite magmas. The association of carbonatite and ijolite within large alkaline complexes is well established (Morogan 1994) and this association proves problematic when attempting to ascertain the source of the fenitizing fluids. Morogan (1994), together with other workers, e.g. Garson et al. (1984) and Morogan and Woolley (1988), cite evidence indicating that fenites develop in both carbonatite-absent and carbonatite-present situations. A study of the Alnö carbonatite complex by Morogan and Woolley (1988) documented the development of different fenite varieties through two main types of fluid, which were related to two different magmatic sources: carbonatitic and ijolitic. This implies that two independent sources of fenitizing agent were active, with different characteristics, reflecting the different compositions of the magma driving the alteration. Le Bas (1987) proposed that fenites associated with ijolite intrusions form via water-rich fluids derived during the fractionation of a nephelinite magma towards ijolitic composition at high temperatures (>700 °C). The high temperatures are reflected by the compositions of feldspars (commonly $Or_{40–60}Ab_{60–40}$). The compositions of alkali feldspar (almost pure albite: $Ab_{>90}$ or orthoclase: $Or_{>85}$) typical of fenites around carbonatites reflect much lower temperatures of fenitization (below 550 °C), commonly involving fluids rich in CO_2. In the case of fenites associated with ijolitic magmas, mineralogical zonation (Fig. 1) is pronounced within the metasomatic aureole. Pyroxene grades from weakly sodic aegirine–augite near the aureole–country rock contact to almost pure aegirine in the aureole zone closest to the intrusion. Feldspar produced near the aureole–intrusion contact is usually hypersolvus alkali feldspar and original subsolvus feldspars of the country rock survive in the outer zones. Fenites produced around carbonatite intrusions seem to be more varied in character. Fenitization in this case is almost exclusively developed in association with sövites, dolomitic carbonatites and rarely microsövites. Depth of emplacement and, therefore, vertical temperature gradients, are important when considering fenitization associated with carbonatite. The uppermost parts of sövites are characterized by strongly potassic alteration along with the formation of pure K-feldspar lithologies ($Or_{>85}$). In older more deeply eroded examples, feldspathic fenites developed around sövites are albite rich ($Ab_{>90}$).

The nature of the fenitizing fluid

Most studies on fenites and fenitization have focused on the changes in mineralogy and chemistry resulting from the metasomatic process, or attempt to model the chemical changes observed in natural examples where the protolith is well defined (e.g. Gresens 1967; Grant 1986). Few studies constrain the compositions of the fluid phases that produce fenite alteration, especially that associated with alkali-silicate magmas. Primary fluid and solid inclusions from carbonatites have been used in an attempt to constrain the chemistry of fenitizing solutions associated with these magmas. However, these studies have produced no widely applicable results (e.g. Andersen 1986; Morogan and Lindblom 1995; Samson et al. 1995). Experimental investigations can successfully constrain the composition of fluids in equilibrium with felsic magmas, and the direct measurement of fluid compositions is possible if the problem of fractionation of the chemistry of the fluid via the precipitation of quench phases upon quenching can be overcome. Studies on granites indicate that at least two different techniques are possible. London et al. (1988) used a double capsule technique to constrain elemental partitioning in granite pegmatite systems using a rhyolite stating composition, and demonstrated that the

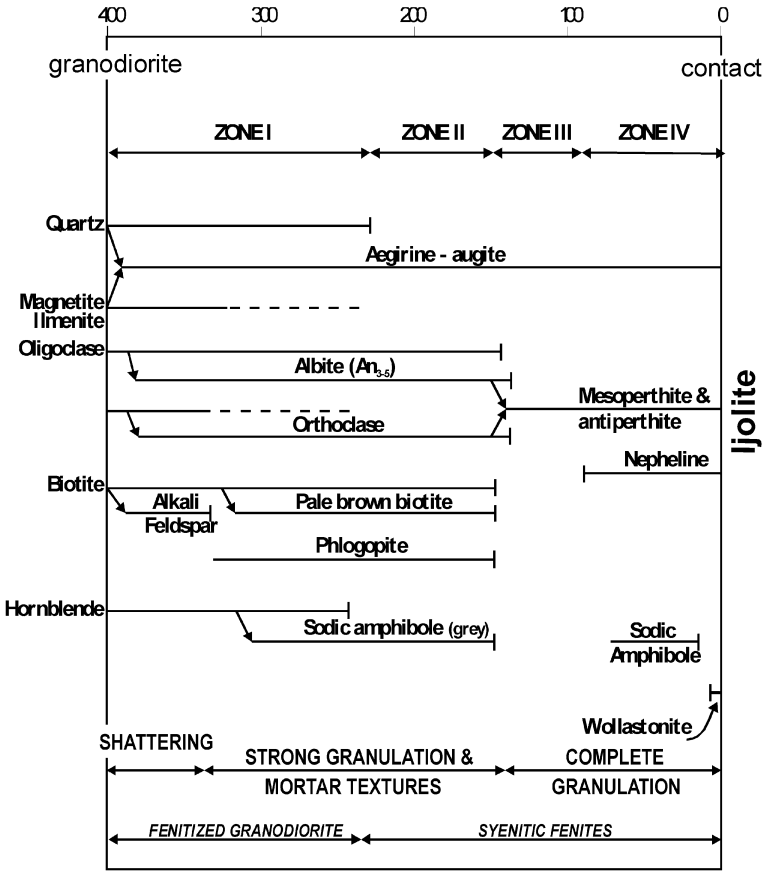

Fig. 1 Mineralogical changes during progressive fenitization of a granodiorite intruded by ijolite (after Le Bas 1987)

solubility of rock components in the fluid ranged from 15 to 9% over the temperature range 775 to 600 °C. Bai and Koster van Groos (1999) investigated elemental partitioning between a granitic melt and fluid phase using a single capsule approach and demonstrated significant solubility of rock components, similar to the findings of London et al. (1988), in water-rich fluids under the conditions of their experiments. Only a single previous study has attempted to analyse possible fenitizing fluid compositions via an experimental approach. In their study of fluid compositions in equilibrium with carbonatite magmas, Veksler and Keppler (2000) adopted a double capsule technique similar to that of London et al. (1988). In their experiments, a perforated inner capsule separates a carbonate powder from diamond powder and water contained in the outer capsule at the beginning of the experiment, the rationale being that the carbonatite magma stays in the inner capsule with the aqueous fluid predominantly contained in the porous diamond powder in the outer capsule. Thus, the fluid composition can be measured by analyzing a solution derived from dissolution of the entire contents of the outer capsule (excluding diamond), thereby overcoming the problem of solid phases precipitating from the high-temperature fluid during quenching of the experiment. Their results successfully quantified elemental partitioning for Mg, Ca and Na in the synthetic system $CaO–MgO–Na_2O–CO_2–H_2O$ and typical fluids in their experiments at 850 °C and 1 to 2 kbar were strongly enriched in rock-forming components (typically –15.2% $MgCO_3$, 24.2 wt% $CaCO_3$, 60.6 wt% Na_2CO_3) highlighting the potential of fluids derived from this source as agents of metasomatism.

Experimental methods

In reconnaissance experiments conducted using a similar double capsule approach to that used Veksler and Keppler (2000) small beads of glass, identical in composition to the glass, developed in both the inner capsule and the outer capsule. This is perhaps not surprising if it is considered that, at equilibrium, the fluid is a supercritical solution, saturated with respect to the chemical components of the magma. Thus, magma may be able to form at any point in the fluid, and will be particularly favoured to do so at any position in the outer capsule with a slightly lower temperature. We concluded that small proportions of the magma incorporated into the outer capsule by this mechanism would have made reliable estimation of the composition of the high-temperature fluids impossible. Consequently, a single capsule mass-balance approach was adopted for determining the fluid composition, which relies on accurate separation of the magma and fluid-derived products in the quenched experimental charges. Using this capsule

configuration, the melt and fluid are able to equilibrate completely during the experiment, and the distribution of the two phases within the single capsule is unambiguous. The mass of the fluid in the capsule at the run condition can be calculated by difference from the mass of glass (melt) retrieved from the capsule and the mass of starting components (oxide powder + deionized water):

$$\text{mass of starting powder} = \text{mass of melt} + \text{mass of fluid} \quad (1)$$

If the mass of glass and fluid, as well as the compositions of the starting mixture and glass, are known, the concentration of any component in the fluid can be calculated via the relationship:

$$\%\,X \text{ in starting powder} \times \text{mass of starting powder} = \%X \text{ in melt} \times \text{mass of melt} + \%X \text{ in fluid} \times \text{mass of fluid} \quad (2)$$

where X is either SiO_2, Al_2O_3, Na_2O or H_2O.

Experimental apparatus

Experiments were carried out in René 42 or Inconel cold seal pressure vessels. The René 42 vessels have an internal diameter (i.d.) of 6 mm, an outside diameter (o.d.) of 25 mm and a length of 203 mm. Inconel vessels have an i.d. of 6 mm, an o.d. of 30 mm and a length of 250 mm. More detailed reviews of this type of equipment are provided by Edgar (1973) and Kerrick (1987). All experiments were run with the vessels in a vertical position, using de-ionised water as the pressure medium. Confining pressures were monitored via a HEISE bourdon tube gauge and pressure was stable to ± 10 bar during the course of each experiment. Temperature measurement was via a type K thermocouple located in a measuring port machined into the outside of the pressure vessel, directly adjacent to the sample capsule, and a Temperature Controls solid state temperature controller with integral ice point. The temperature of the external tube furnace was measured and controlled by an identical device. Temperatures at the sample capsule were readily maintained within 1 °C of the set point for the duration of an experiment. The temperature gradients between the inside of the vessel at the hotspot and the thermocouple well, as well as along the sample length, were determined using two internal and one external thermocouple in a dummy run at 850 °C and 1,000 bar. Under these conditions, the temperature gradient over the sample volume was approximately 3 °C and a temperature difference of 1 °C existed between the average temperature across the sample volume and the external thermocouple well. Thus, temperature measurements during the experiments are believed to be accurate to ± 2 °C over the capsule length ($\approx$20 mm).

All experiments were carried out at conditions of 850 °C and 1,000 bar, for periods no shorter than 120 h, followed by isobaric quenching. Runs using Inconel vessels required < 2 min to cool from 850 to 450 °C and a further 8 min to cool from 450 to 150 °C. Runs using the smaller René 42 vessels cooled in approximately half these times. Experiments were conducted either in platinum or gold capsules, sealed by arc welding with a graphite electrode. The capsules typically have a wall thickness of 0.2 mm, a length of 20 mm and an internal diameter of 2.93 mm.

Starting materials

The starting materials used in this study were synthesized from high purity powders of aluminum oxide (Al_2O_3), sodium carbonate (Na_2CO_3) and silicon dioxide (SiO_2). These compounds were carefully dried and mixed in the desired molar proportions, homogenized using a pestle and mortar and fused in a platinum crucible at 1,000 °C. During this process Na_2CO_3 completely decomposed to Na_2O, thus precluding the incorporation of any CO_2 into the starting materials. The resultant anhydrous glass was ground to a fine powder (approximately 5 μm grain size) in preparation for use in the experiments, re-dried at high temperature and kept in a desiccator, under vacuum, prior to use. Twenty-five starting compositions were prepared in this manner. These compositions straddle the nepheline–albite join and include peralkaline and alkaline granitoid compositions (Fig. 2). Starting compositions were loaded into noble metal capsules with approximately 40 wt% deionized water.

Analytical techniques

The compositions of the quenched glasses were determined using the JEOL Superprobe 733 electron microprobe at the Council for Geoscience, Pretoria, using an accelerating voltage of 15 keV, a beam current of 1.9808×10^{-8} A and analysis spot size of 20 μm. This relatively low energy beam and defocused spot were used to counter the decline in sodium counts over the course of an analysis that is typical for sodium-rich aluminosilicate glasses. Instrument calibration was done using natural mineral standards, and checks for the accuracy of Na concentration were carried out using SiO_2, Al_2O_3 and Na_2O natural glass standards (NBS 620 and 621; Table 1). The ZAF correction procedure was employed. The mineralogy of crystal-bearing glasses was confirmed by semi-quantitative EDS analysis, using a NORAN EDS attached to the JEOL JSM-5600 scanning electron microscope at Rand Afrikaans University, Johannesburg, with an accelerating voltage of 15 kV and a counting time of 100 s. Backscattered and secondary electron SEM images of the run products were generated with this same instrument.

Experimental results

Twenty-six experiments were carried out. Recovered capsules were weighed, checked for weight loss or gain and, if they had not leaked, carefully opened. Solid and liquid run products were extracted by washing all the run products out of the capsule with deionized water and careful filtration. The interiors of the opened capsules were carefully examined under binocular microscope to confirm that no run products remained

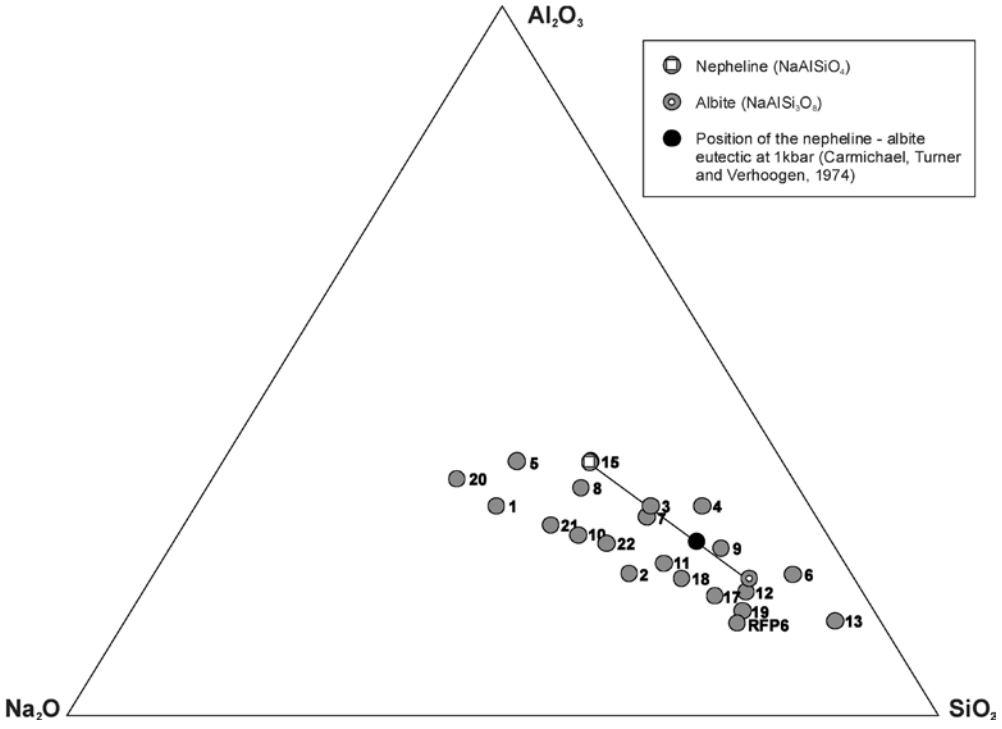

Fig. 2 The ternary system Na_2O–Al_2O_3–SiO_2 (wt%), showing the positions of the 21 starting compositions used in this study. The position of the nepheline–albite eutectic at 1 kbar (Carmichael et al. 1974) is also shown

Table 1 A comparison of the measured and actual compositions of the glass standard used for calibration of the JEOL Superprobe 733 electron microprobe

	NBS 620		NBS 621	
	Standard	Measured value	Standard	Measured value
SiO_2	72.08	72.121	71.130	71.397
TiO_2	0.018	0.026	0.014	0.019
Al_2O_3	1.800	1.924	2.760	3.007
ZrO_2	–	–	0.007	–
Cr_2O_3	–	0.000	–	0.000
Fe_2O_3	0.043	0.008	0.040	0.008
MnO	–	0.000	–	0.035
MgO	3.690	4.062	0.270	0.271
CaO	7.110	7.343	10.710	10.912
BaO	–	–	0.120	–
Na_2O	14.390	13.934	12.740	12.607
As_2O_3	0.056	–	0.030	–
SO_3	0.280	–	0.130	–
Total	99.880		99.960	

adhering to the capsule walls. All experiments produced a translucent isotropic glass representing the quenched melt, as well as solid products interpreted to have precipitated from the fluid phase during cooling (Table 2). In several cases the glasses contain inclusions of nepheline or albite. In general, these occur as euhedral crystals (Figs. 3 and 4) and are interpreted to be stable phases in the high temperature assemblage, not quench products. In most cases the glass had fragmented during quenching and opening of the capsule and was present as chunks and shards with obvious concoidal fracture. In nine experiments, homogeneous, crystal-free glass was produced (Table 2, Fig. 3a–c). Generally, experiments with starting compositions plotting on the peralkaline side of the nepheline–albite join produced homogeneous, crystal-free quenched glasses, while those with starting compositions near the nepheline–albite tie line, and in the alkaline granitoid field, produced crystal-bearing glasses. The portion of the solid products interpreted to have formed as quench products from the fluid phase occurs as crystalline beads with a radial internal structure (Figs. 3a and 4d). In some cases these are relatively coarsely crystalline and appear to have formed above the solidus as they produce indentations in the glass (Fig. 3a). In other experiments, the radial quench crystals are considerably finer grained and in these experiments no glass indentations are noted, presumably reflecting precipitation from the fluid under sub-solidus conditions (Fig. 4d). The dried, solid run products were separated, by grain picking under a binocular microscope, into the glass and fluid phase quench product fractions. Although time consuming, this was relatively easy to do as the process was facilitated by the anisotropic nature of the fluid phase quench products. Large pieces of glass with adhering fluid phase quench products were carefully broken up to allow them to be properly separated. The separated fluid phase quench products and glass were accurately weighed.

Equation (2) can only be applied to experiments run at conditions above the liquidus. Melt compositions (determined by EMPA) from the glasses produced in these experiments are presented in Table 3. Four duplicate runs were conducted for experiments that produced crystal-free quenched glasses, three with high silica (S2a and S2b; S12a and S12b; and S18a and S18b)

Table 2 Starting conditions and experimental products. All runs were conducted at 850 °C and 1,000 bar for periods no shorter than 120 h. *Gl* Glass; *FQP* fluid quench phase; *Fl* fluid; *Nep* nepheline; *Ab* albite; *MQP* melt quench phase; *Qtz* quartz

Run no.	Initial run charge		Run compositions				Run products
	(g)		(wt%)				
	Solid	H_2O	SiO_2	Al_2O_3	Na_2O	H_2O	
S1a	0.12301	0.04230	18.01	15.28	18.58	48.12	Gl + FQP + Fl
S1b	0.04556	–	18.01	15.28	18.58	~48	Gl + FQP + Fl
S2a	0.10640	0.07442	32.13	11.81	14.91	41.15	Gl + FQP + Fl
S2b	0.04047	0.02838	32.08	11.79	14.89	41.24	Gl + FQP + Fl
S3	0.08773	0.07425	28.35	16.04	9.75	45.86	Nep + Gl + Fl
S4a	0.10508	0.07439	34.14	17.37	7.04	41.45	Ab + Gl + FQP + Fl
S4b	0.04140	0.02938	34.09	17.35	7.03	41.53	Ab + Gl + FQP + Fl
S5	0.07575	0.07387	17.09	18.12	15.42	49.37	Nep + Gl + FQP + Fl
S6	0.08736	0.07649	39.16	10.71	3.46	46.67	Gl + MQP + FQP + Fl
S7	0.09114	0.07379	29.12	15.56	10.56	44.75	Nep + Gl + FQP + Fl
S8a	0.08237	0.06498	24.19	18.08	13.91	43.83	Nep + FQP + Fl
S9	0.04109	0.04481	30.33	11.32	6.21	52.15	Ab + Gl + FQP + Fl
S10	0.04117	0.03662	24.42	13.47	15.07	47.04	Gl + FQP + Fl
S11	0.03881	0.03510	30.42	11.30	10.78	47.50	Nep + Gl + FQP + Fl
S12a	0.03958	0.03847	35.13	8.90	6.67	49.30	Gl + FQP + Fl
S12b	0.03987	0.03499	36.91	9.35	7.01	46.73	Gl + FQP + Fl
S13	0.04078	0.03404	44.47	7.42	2.65	45.45	Qtz + Gl + FQP + Fl
S15	0.04028	0.03016	24.18	20.52	12.47	42.84	Nep + Gl + FQP + Fl
S17	0.04066	0.02980	38.03	9.86	9.81	42.29	Nep + Gl + FQP + Fl
S18a	0.04134	0.02918	34.99	11.57	11.57	41.90	Gl + FQP + Fl
S18b	0.00712	0.0068	30.47	10.08	10.08	49.39	Gl + FQP + Fl
S19	0.03834	0.02982	39.53	8.39	8.34	43.73	Nep + Gl + FQP + Fl
S20	0.03891	0.01418	20.67	24.46	28.13	26.74	Nep + Gl + FQP + Fl
S21	0.02973	0.01979	25.36	16.14	18.52	39.98	Nep + Gl + FQP + Fl
S22	0.02783	0.01858	29.96	14.53	15.45	40.06	Nep + Gl + FQP + Fl

and the other with low silica (S1a and S1b). The reproducibility of melt composition in the duplicate experiments, including that of water content, which is determined by difference, is good (Table 3).

The composition of equilibrium fluids

Fluid compositions were calculated for the data listed in Tables 2 and 3 using Eq. (2). The results are listed in Table 4, and indicate between 40 and 50 wt% dissolved rock components ($Na_2O + Al_2O_3 + SiO_2$) in the fluids, i.e. the fluids are remarkably concentrated. Fluid composition could not be calculated for S1a as the amount of water added to the capsule had not been accurately recorded. That in S2a could not be calculated as glass and quenched fluid products could not be satisfactorily separated. There is good agreement between the calculated fluid compositions for duplicate experiments (Table 4). The calculated fluid compositions, measured melt and starting compositions are plotted in tetrahedral space; SiO_2–Al_2O_3–Na_2O–H_2O (Fig. 5). The equilibrium melt and fluid compositions define two surfaces (albeit with some scatter) that appear to be part of a single solvus. With decreasing silica content of the starting composition, these surfaces approach one another and suggest that the melt and fluid phases may become completely miscible at very low silica contents. The proportion of sodium and aluminium in the fluid increases with decreasing silica content in the melt, suggesting that the fluids derived from more strongly silica undersaturated magmas should be more efficient fenitizing agents.

Sources of error in the calculated fluid compositions

The sources of error in the calculated fluid compositions are:

1. The mass of the glass extracted from the capsule. This affects the values for the masses of both melt and fluid used in the mass balance calculation and underestimating mass of the glass fraction increases the dissolved solids content of the calculated fluid phase. Consequently, great care was taken to make sure no glass fragments were left in the fraction assigned to fluid phase quench products. In order to do this it was accepted that minor quantities of fluid quench products be included in the glass fraction, generally as very small pieces stuck to the surface of pieces of glass. The mass of the glass is also likely to be slightly overestimated as a result of the occurrence of fluid inclusions within the glass. The combined errors this induced are estimated to be in the range of ± 2 to 5% of the determined value for the mass of the glass. Fluid compositions were recalculated with a 10% relative uncertainty on the mass of the glass recovered

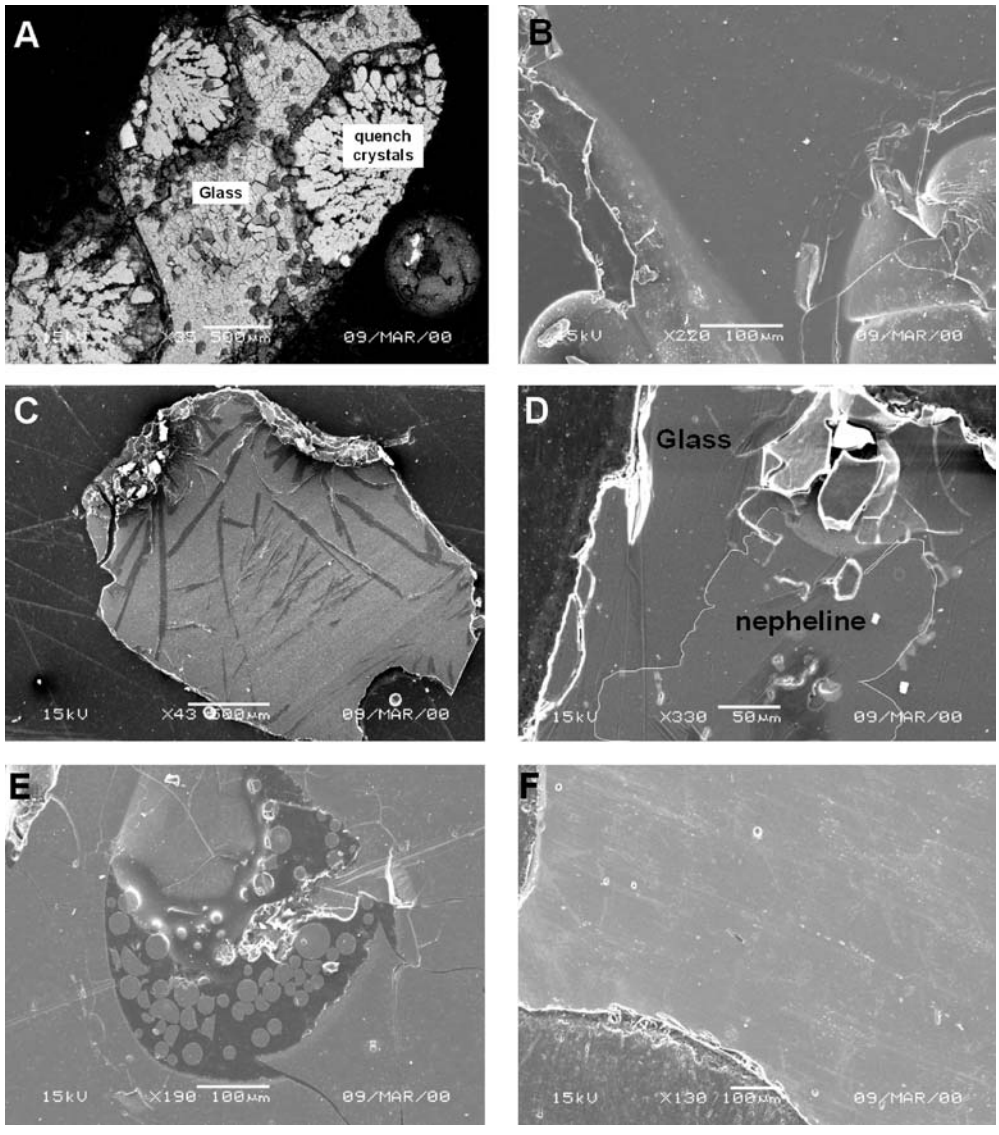

Fig. 3A–F Scanning electron microscope images of typical run product textures, all taken in secondary electron mode, except for **A** taken in backscattered electron mode. **A** Glass representing quenched melt and radial crystals derived from the fluid phase during quenching experiment S1a; **B** typical appearance of homogeneous, crystal-free glass from experiment S2b; **C** uncommon occurrence of acicular crystals within the glass formed through devitrification of the quenched glass experiment S2a; **D** nepheline crystals in the glass experiment S11; **E** glass beads with the same composition as the large encircling fragment of glass from experiment S12b. In reconnaissance double capsule experiments, these were found in both the inner and outer capsules, prompting the experimental design used in this study; and **F** homogeneous, crystal-free glass from experiment S18a, close to the Ne–Ab eutectic

from the capsule (Fig. 6a). The results indicate that the variation this induces in the calculated fluid compositions is greatest in the least concentrated fluids, and that all fluids remain strongly concentrated in rock-forming elements.

2. Analytical uncertainties in the determination of the Na_2O concentration in the glasses – underestimation of this value will result in incorrectly high Na_2O concentrations in the calculated fluid compositions. Na_2O is typically difficult to measure accurately in hydrous aluminosilicate glasses as sodium counts decline during the course of an analysis. An attempt was made to counter this by standardizing on an appropriate glass composition and choosing an analytical setup likely to reduce the problem. However, the composition of the standard corresponds most closely to the least hydrous and Na_2O-rich glass compositions produced in these experiments, and the degree of Na_2O underestimation is known to increase as a function of both the water and Na_2O content of the glass. Consequently, a glass control standard was synthesized with a composition more closely approaching that of the most Na_2O- and H_2O-rich glasses produced in the experiments ($SiO_2 = 53$ wt%, $Al_2O_3 = 21$ wt% $Na_2O = 17$ wt% and $H_2O = 9$ wt%). Analysis of this glass, with the same setup as used for the unknowns, indicated that Na_2O concentration in these compositions may be underestimated by as much as 3 wt%. The fluid compositions were recalculated assuming 30% relative underestimation of the Na_2O concentration in all the glasses (the equivalent of a 6 wt% underestimation in the most Na_2O-rich glasses). The results (Fig. 6b) indicate that the calculated fluid compositions are shifted to less Na_2O rich compositions, but remain strongly concentrated in all elements including Na_2O.
3. Water content of the glasses. In this study, spot analyses were carried out where the surface of the quenched hydrous melt was homogeneous, and free of vesicles or fluid inclusions (as determined by

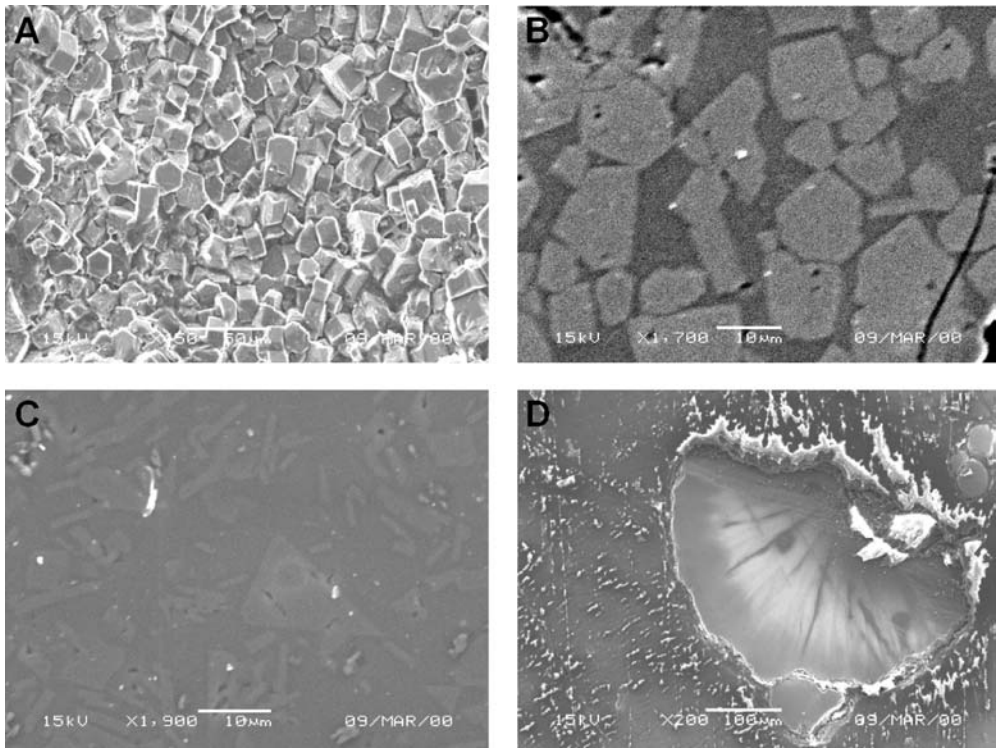

Fig. 4A–D Scanning electron microscope images (all in secondary electron mode) of equilibrium mineral phases and quench products developed in the run products. **A** Hexagonal nepheline crystals exhibiting a cumulus texture in experiment S8b, with a bulk composition close to that of nepheline; **B** nepheline crystals as inclusions in glass from experiment S3; **C** euhedral albite crystals as inclusions in glass from experiment S9; **D** a radially crystalline quench bead formed during isobaric quenching of the fluid phase in experiment S1b

Table 3 Average composition (wt%) of the glasses as determined by EMPA. *n* Number of analysis points; *SD* standard deviation. (H_2O content was calculated by difference from the anhydrous total.) It is clear from the table that the largest relative uncertainties are for Na_2O and H_2O. The compositions in *italics* were not used in the fluid composition calculations because in the case of S1b, the amount of water added to the capsule was not accurately recorded and, in the case of S2a, the glass and fluid phase quench products could not be satisfactorily separated

Run no.	SiO_2	S	Al_2O_3	S	Na_2O	S	H_2O	SD	*n*
S1a	38.35	0.63	31.56	1.05	19.29	2.17	10.80	1.54	9
S1b	*35.50*	*1.03*	*3165*	*1.11*	*20.91*	*2.43*	*11.88*	*1.77*	*11*
S2a	*51.39*	*0.65*	*20.53*	*0.52*	*19.87*	*0.79*	*8.22*	*1.72*	*24*
S2b	54.82	0.61	21.92	0.44	13.03	1.65	10.24	1.74	35
S6	73.65	0.31	15.11	0.22	4.54	0.43	6.67	1.02	9
S10	45.50	0.65	23.99	1.10	21.81	2.10	8.43	1.75	14
S12a	66.60	1.28	17.14	0.51	8.74	1.47	7.51	0.37	20
S12b	66.17	2.22	16.79	0.63	8.75	1.29	7.91	2.54	33
S18a	59.73	0.81	22.52	0.51	12.07	0.23	5.72	0.81	76
S18b	59.23	0.38	24.56	0.24	11.16	0.08	5.09	0.56	17

transmitted light microscopy). The derived water contents of the glasses are relatively high and show a strong compositional dependency, with apparent water content increasing with decreasing silica content of the melt (Fig. 7). McMillan and Holloway (1987) compiled water solubility data from a number of previous investigations for an extensive range of natural and synthetic aluminosilicate melts. They have shown that systematic variations in melt water solubility exist as a function of composition and that high water solubilities are associated with alkaline systems as opposed to alkaline earth silicate melts. Figure 7 compares the data for this study with data on the solubility of water in melts of albite and nepheline composition, as compiled by McMillan and Holloway (1987), and demonstrates that although the glass water contents documented in this study are high, they are comparable with those documented on some similar, but not identical compositions in previous studies, which were conducted at substantially higher temperatures. The calculated fluid compositions are generally insensitive to melt water content, and reducing the melt water contents by 3 wt% typically increases the water content of the calculated fluid compositions by less than 1 wt%.

Modeling the fenitization process

The capacity of the previously calculated fluid compositions to metasomatize granitoid rocks can be evaluated

Table 4 Calculated equilibrium fluid compositions. All values are in wt%

Run no.	SiO_2	Al_2O_3	Na_2O	H_2O
S1a	15.3	13.2	18.5	52.9
S2b	19.3	6.1	15.9	58.4
S6	19.0	8.1	2.8	70.0
S10	21.4	11.9	14.1	52.4
S12a	23.6	5.9	5.9	64.8
S12b	22.28	5.6	6.1	65.9
S18a	19.7	4.9	11.2	63.2
S18b	19.2	4.5	9.6	65.9

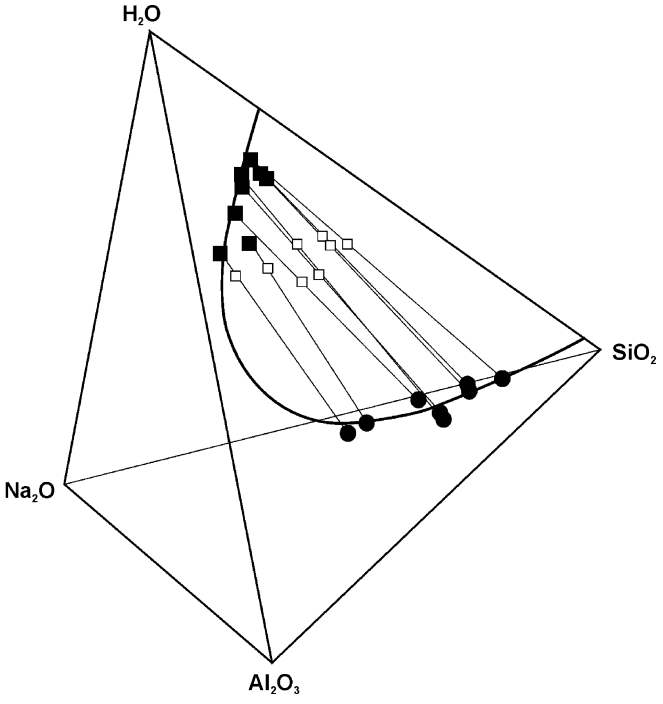

Fig. 5 Compositions of the starting mixtures, glasses and calculated equilibrium fluids, plotted in the tetrahedral system SiO_2–Al_2O_3–Na_2O–H_2O (wt%). The *fine lines* represent tie lines linking starting compositions (*white squares*) with melt compositions (*black circles*) and calculated fluid compositions (*black squares*). The *heavy gray line* represents the continuous solvus that may exist in the system

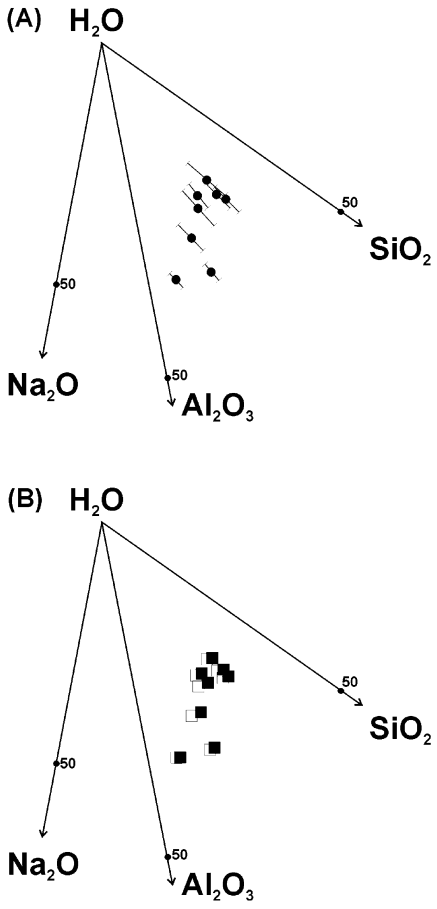

Fig. 6 **A** Calculated fluid composition error resulting from a 10% over and underestimation of the mass of glass in the capsules. Fluid compositions derived from the more SiO_2-rich magmas are most strongly affected because of the more dilute nature of these fluids. **B** The error in fluid composition that results from a 30% underestimation of the Na_2O concentration in the glasses. The *white squares* represent the fluid compositions calculated with the glass compositions measured in this study, the *black squares* represent the fluid compositions calculated assuming 30% more Na_2O in the glass

by considering the quantity of fluid required to convert a typical granitoid composition to that of a nepheline normative rock. This was done by calculating the CIPW norms of mixtures of a typical granodiorite from the Archaean basement of the Kaapvaal Craton with different proportions of fluid compositions S18b, S10 and S1a (Fig. 8). The model is simplistic, as the fluid is seen to add its entire composition to the metasomatized product, without dissolving and removing chemical components from the granitoid. In this process, fluid composition S18b that equilibrated with a relatively SiO_2-rich magma, does not produce a nepheline normative result in any combination with the protolith. In contrast, fluid compositions S10 and S1b, which equilibrated with relatively SiO_2-poor magmas, produce a nepheline normative result when combined with the granodiorite in fluid:rock ratios of between 1:2 and 1:1, by weight. The norm calculations involving these fluid compositions suggest that at very low fluid rock ratios, the metasomatic process manifests itself as a reduction in normative quartz, increase in normative albite, the formation of acmite and the appearance of diopside at the expense of anorthite. At a slightly higher fluid:rock ratio, sodium metasilicate appears in the norm and increases in quantity, together with albite, while normative quartz decreases. At a fluid rock ratio of approximately 0.8:1 nepheline appears in the result for fluid S1b. This sequence is in many ways analogous to what is observed in fenite aureoles (e.g. Le Bas 1987) in that the early stages of fenitization are characterized by the formation of alkali pyroxene (acmite in the norm), reduction and eventual disappearance of quartz, increase in alkali

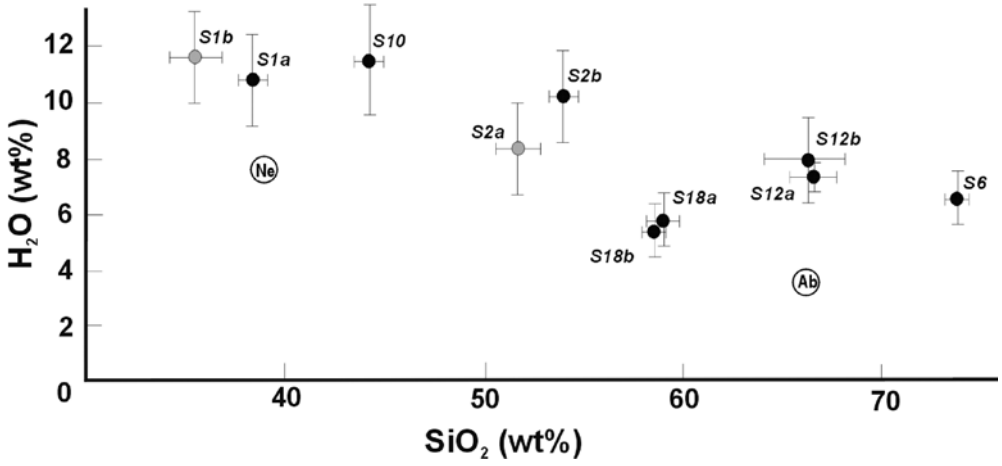

Fig. 7 Binary plot of average SiO_2 vs. H_2O (in wt%) in the glasses, showing the systematic variation of water content with respect to SiO_2 in the glass. The *grey points* represent measured glass compositions from successful experiments above the relevant liquidus that were not used in the fluid composition calculations for the reasons explained in the text. The points Ne and Ab represent water solubility at 1 kbar in glasses of nepheline and albite composition, respectively, as complied by McMillan and Holloway (1987). The *error bars* represent twice the standard deviation values listed in Table 3

feldspars, disappearance of anorthite, the appearance of diopsidic pyroxene and the disappearance of hematite (see Fig. 1). The reduction in quartz is most likely due to two processes: one being a conversion to alkali pyroxene (acmite) and the other, its dissolution back into the fluid phase as a sodium meta-silicate component.

Concluding remarks

The melts produced in this study are in equilibrium with fluids that contain very large proportions of dissolved solids (SiO_2, Al_2O_3 and Na_2O), in the range 40–50 wt%, and the fluid and melt compositions possibly define a single solvus surface. Melt compositions plotting towards nepheline on the nepheline–albite join are in equilibrium with fluids that are capable of converting a granite to a nepheline normative composition (nepheline syenite) at low fluid:rock ratios, whereas compositions towards the albite side of the join require very large fluid:rock ratios to accomplish this, or cannot produce nepheline normative compositions at all. This is consistent with field observations. Small alkaline complexes of the ijolite–melteigite series have large metasomatic aureoles in relation to their size, whereas syenitic intrusions appear not to produce sizable aureoles. Simple modeling of the metasomatic process suggests a paragenetic sequence of alteration very similar to those observed in fenite aureoles. The experiments carried out here are not wholly representative of the natural fluids responsible for fenitization, as the natural systems reflect development under far more complex physical and chemical conditions than investigated in this study. Particularly K_2O, Fe_2O_3 and MgO are important additional mobile elements during fenitization. CO_2 may be a major constituent of the fluid phases that will impact on solubility of rock components in the fluid, as well as on the physical properties of the fluid. In addition, minor components within the fluid, such as Cl, have potential to strongly affect the solubility of the rocks components modeled here. Despite these limitations, this study has

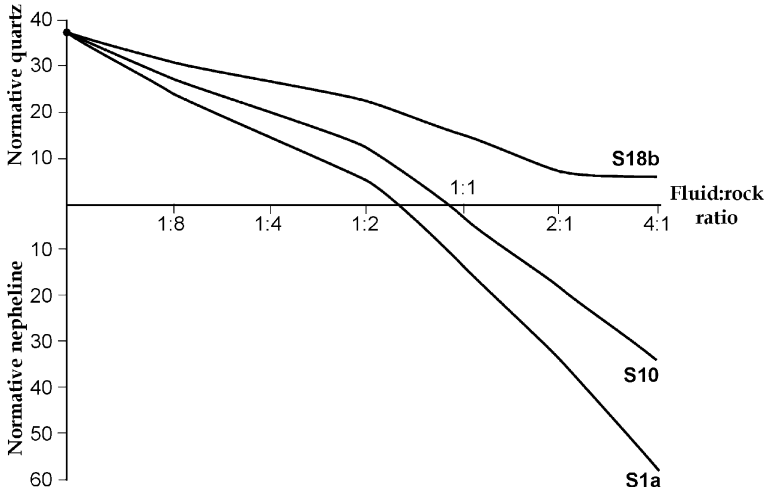

Fig. 8 An illustration of the fenitization potential of the four calculated fluid compositions when reacted with a typical granodiorite composition. Normative quartz and nepheline for the resultant, altered compositions are shown together with the fluid–rock ratios calculated in weight proportions

demonstrated that the fluids in equilibrium with broadly syenitic magmas can contain surprisingly high concentrations of rock-forming components and that given suitable magma compositions, these components are present in the correct proportions to effect metasomatism on granitoid rocks that is consistent with observations in natural fenites.

Acknowledgements The authors wish to thank Dr D. de Bruin and Mrs A. Walliser of the Council for Geoscience, Pretoria, for their assistance during electron microprobe analysis of the glasses. This study was supported by the National Research Foundation and formed the basis of an MSc thesis by R.F.P. This manuscript was improved by helpful reviews from R.E. Harmer, D. London and an anonymous reviewer.

References

Andersen T (1986) Magmatic fluids in the Fen carbonatite complex, SE Norway: evidence of mid-crustal fractionation from solid and fluid inclusions in apatite. Contrib Mineral Petrol 93:491–503

Appleyard EC, Woolley AR (1979) Fenitization: an example of the problems characterizing mass transfer and volume changes. Chem Geol 26:1–15

Bai TB, Koster van Groos AF (1999) The distribution of Na, K, Rb, Sr, Al, Ge, Cu, W, Mo, La and Ce between granitic melts and coexisting aqueous fluids. Geochem Cosmochim Acta 63:1117–1131

Brögger WC (1921) Die Eruptivgesteine des Kristianiagebeites, IV., Das Fengebeit in Telemark. Selsk Vidensk Selsk Skrifter I Math Naturv Kl (1920)9:1–408

Carmichael ISE, Turner FJ, Verhoogen J (1974) Igneous petrology. International Series in Earth and Planetary Sciences. McGraw-Hill, New York

Cooper AF (1971) Carbonatites and fenitization associated with a lamprophyric dike-swarm intrusive into schists of the New Zealand geosyncline. Bull Geol Soc Am 82:1327–1340

Currie KL (1971) A study of potash fenitization around the Brent crater, Ontario: a Paleozoic alkaline complex. Can J Earth Sci 8:481–517

Currie KL, Ferguson J (1971) A study of fenitization around the alkaline carbonatite complex at Callander Bay, Ontario. Can J Earth Sci 8:498–517

Currie KL, Ferguson J (1972) A study of fenitization in mafic rocks, with special reference to the Callander Bay Complex. Can J Earth Sci 9:1254–1261

Currie KL, Knutson J, Temby PA (1992) The Mud Tank carbonatite complex, central Australia – an example of metasomatism at mid-crustal levels. Contrib Mineral Petrol 109:326–339

Edgar AD (1973) Experimental petrology: basic principles and techniques. Oxford University Press, Oxford

Garson MS, Coats JS, Rock NMS, Deans T (1984) Fenites, breccia dykes, albitites, and carbonatitic veins near the Great Glen Fault, Inverness, Scotland. J Geol Soc Lond 141:711–732

Gittins J (1989) The origin and evolution of carbonatite magmas. In: Bell K (ed) Carbonatites: genesis and evolution. Unwin Hyman, London, pp 580–600

Grant JA (1986) The isocon diagram – a simple solution to Gresens' equation for metasomatic alteration. Econ Geol 81:1976–1982

Gresens RL (1967) Composition–volume relationships in metasomatism. Chem Geol 2:47–65

Kerrick DM (1987) Cold-seal systems. In: Ulmer GC, Barnes HL (eds) Hydrothermal experimental techniques. Wiley, New York, pp 292–323

Kresten P (1988) The chemistry of fenitization: examples from Fen, Norway. Chem Geol 68:329–349

Kresten P, Morogan V (1986) Fenitization at the Fen Complex, southern Norway. Lithos 19:27–42

Le Bas MJ (1987) Nephelinites and carbonatites. In: Fitton JG, Upton BGJ (eds) Alkaline igneous rocks. Geol Soc Spec Publ 30:53–83

London D, Hervig RL, Morogan GB (1988) Melt–vapor solubilities and elemental partitioning in peraluminous granite–pegmatite systems: experimental results with Macusani glass at 200 MPa. Contrib Mineral Petrol 99:360–373

McKie D (1966) Fenitization. In: Tuttle OF, Gittins J (eds) Carbonatites. Interscience, New York, pp 261–294

McMillan PF, Holloway JR (1987) Water solubility in aluminosilicate melts. Contrib Mineral Petrol 97:320–332

Morogan V (1994) Ijolite versus carbonatite as sources of fenitization Terra Nova 6(2):166–176

Morogan V, Lindblom S (1995) Volatiles associated with the alkaline-carbonatite magmatism at Alnö, Sweden: a study of fluid and solid inclusions in minerals from the Langarsholmen ring complex. Contrib Mineral Petrol 122:262–274

Morogan V, Woolley AR (1988) Fenitization at the Alnö carbonatite complex, Sweden; distribution, mineralogy and genesis. Contrib Mineral Petrol 100:169–182

Pearson JM, Taylor WR (1996) Mineralogy and geochemistry of fenitized alkaline ultrabasic sills of the Gifford Creek Complex, Gascoyne Province, Western Australia. Can Mineral 34:201–219

Robins B (1984) Petrography and petrogenesis of nephelinized gabbros from Finnmark, Northern Norway. Contrib Mineral Petrol 86:170–177

Robins B, Tysseland M (1983) The geology, geochemistry and origin of ultrabasic fenites associated with the pollen carbonatite (Finnmark, Norway). Chem Geol 40:65–95

Rubie DC (1982) Mass transfer and volume change during alkali metasomatism at Kisingiri, western Kenya. Lithos 15:99–109

Saether E (1957) The alkaline rock province of the Fen area in southern Norway. K Nor Vidensk Selsk Skr, vol 1

Samson IN, Williams-Jones AE, Liu W (1995) The chemistry of hydrothermal fluids in carbonatites: evidence from leachate and SEM-decrepitate analysis of fluid inclusions from Oka, Quebec, Canada. Geochim Cosmochim Acta 59:1979–1989

Siemiatkowska KM, Martin RF (1975) Fenitization of Mississagi quartzite, Sudbury area, Ontario. Bull Geol Soc Am 86:1109–1122

Sindern S, Kramm U (2000) Volume characteristics and element transfer of fenite aureoles: a case study from the Iivaara alkaline complex, Finland. Lithos 51:75–93

Strauss CA, Truter FA (1950) The alkali complex at Spitzkop, Sekukuniland, Eastern Transvaal. Trans Geol Soc S Afr 53:81–125

Vartiainen H, Woolley AR (1976) The petrography, mineralogy and chemistry of the fenites of the Sokli carbonatite intrusion, Finland. Bull Geol Surv Finland no 280

Veksler IV, Keppler H (2000) Partitioning of Mg, Ca and Na between carbonatite melt and hydrous fluid at 0.1–0.2 GPa. Contrib Mineral Petrol 138:27–34

Verwoerd WJ (1966) South African carbonatites and their probable mode of origin. Ann Univ Stellenbosch Series A 41(2):113–233

Von Eckermann H (1948) The alkaline district of Alnö Island. Sveriges Geol Unders Ca 36:1–176